Electrospun Carbon Nanofiber Modified Electrodes for Stripping Voltammetry

ARTICLE *in* ANALYTICAL CHEMISTRY · AUGUST 2015

Impact Factor: 5.64 · DOI: 10.1021/acs.analchem.5b02017

6 AUTHORS, INCLUDING:

Tingting Wang
University of Texas at Austin
14 PUBLICATIONS **61** CITATIONS
SEE PROFILE

Daewoo Han
University of Cincinnati
22 PUBLICATIONS **217** CITATIONS
SEE PROFILE

Andrew Steckl
University of Cincinnati
421 PUBLICATIONS **6,341** CITATIONS
SEE PROFILE

analytical chemistry

Article

pubs.acs.org/ac

Electrospun Carbon Nanofiber Modified Electrodes for Stripping Voltammetry

Daoli Zhao,[†] Tingting Wang,[†] Daewoo Han,[‡] Cory Rusinek,[†] Andrew J. Steckl,[‡] and William R. Heineman*[,†]

[†]Department of Chemistry, University of Cincinnati, Cincinnati, Ohio 45221-0172, United States

[‡]Nanoelectronics Laboratory, Department of Electrical Engineering and Computing Systems, University of Cincinnati, Cincinnati, Ohio 45221-0030, United States

Supporting Information

ABSTRACT: Electrospun polyacrylonitrile (PAN) based carbon nanofibers (CNFs) have attracted intense attention due to their easy processing, high carbon yield, and robust mechanical properties. In this work, a CNF modified glassy carbon (GC) electrode that was coated with Nafion polymer was evaluated as a new electrode material for the simultaneous determination of trace levels of heavy metal ions by anodic stripping voltammetry (ASV). Pb^{2+} and Cd^{2+} were used as a representative system for this initial study. Well-defined stripping voltammograms were obtained when Pb^{2+} and Cd^{2+} were determined individually and then simultaneously in a mixture. Compared to a bare GC electrode, the CNF/Nafion modified GC (CNF/Nafion/GC) electrode improved the sensitivity for lead detection by 8-fold. The interface properties of the CNF/Nafion/GC were characterized by electrochemical impedance spectroscopy (EIS), which showed the importance of the ratio of CNF/Nafion on electrode performance. Under optimized conditions, the detection limits are 0.9 and 1.5 nM for Pb^{2+} and Cd^{2+}, respectively.

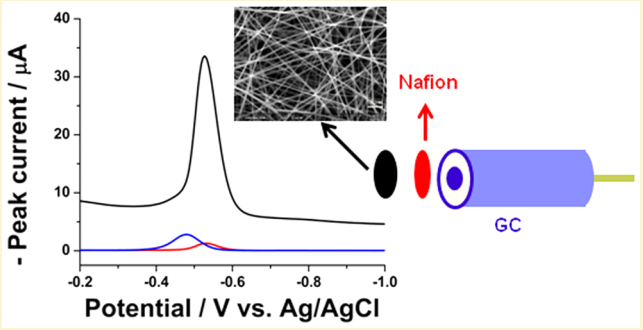

Among the carbon materials, carbon nanofibers (CNFs) have attracted much attention due to their high mechanical strength, large specific surface area, superior stiffness, excellent electrical and thermal conductivities, as well as strong fatigue and corrosion resistance. A simple and effective method to prepare the CNF precursor is by the electrospinning technique. Electrospinning is a fiber formation process using electrical force to generate fibers with diameters on the order of 100 nm. A wide variety of polymers have been used as precursors for CNF preparation. Polyacrylonitrile (PAN) is the most popular one due to high carbon yield, easy processing, and robust mechanical properties of the as-prepared CNFs.[1−3] After thermal treatment including stabilization and carbonization of the PAN precursor, CNFs have been obtained with the desired nanostructural, electrical, and mechanical properties. Because of these distinguishing properties, PAN based CNFs have been used for supercapacitors,[4,5] filters,[6] catalyst for rechargeable batteries,[7,8] and energy storage.[1] Although the reported applications are extensive, to the best of our knowledge, there is no report using PAN based CNFs as an electrode material for heavy metal ion detection by electrochemical methods.

Anodic stripping voltammetry (ASV) is a powerful electroanalytical technique for trace metal measurement.[9−15] It offers the characteristics of high sensitivity, good selectivity, simultaneous multielement determination, simplicity, portability, and relatively low cost. Its remarkable sensitivity is attributed to the combination of the effective preconcentration step with advanced measurement procedures that generate an extremely favorable signal to background ratio by pulsing the potential.[10] For stripping voltammetry, proper choice of the working electrode is crucial. Mercury electrodes (film and drop) have been extensively used due to their high sensitivity, good reproducibility, and superior negative potential limit. However, their use is now restricted because of mercury toxicity and the need for proper disposal of waste mercury. More environmentally friendly bismuth has been used extensively as a substitute for mercury, but it has a relatively narrow potential window.[10] Thus, the development of alternative electrode materials is necessary.

We report here the first use of PAN-based CNF/Nafion modified glassy carbon (CNF/Nafion/GC) to detect heavy metal ions by ASV. Pb^{2+} and Cd^{2+} were used as representative metal ions to evaluate the performance of the CNF/Nafion/GC electrode for ASV because their toxicity causes serious problems in the environment and for human and animal health.[16,17] This work shows the advantages of the CNF/Nafion/GC electrode compared to other reported electrode materials. The CNF/Nafion/GC enhanced the stripping peak current compared to

Received: May 29, 2015
Accepted: August 10, 2015

DOI: 10.1021/acs.analchem.5b02017
Anal. Chem. XXXX, XXX, XXX−XXX

the bare glassy carbon electrode giving higher sensitivity. The electrochemical properties of the modified electrode were investigated by electrochemical impedance spectroscopy (EIS).

EXPERIMENTAL SECTION

Materials and Instrumentation. All chemicals were from Sigma-Aldrich or Fisher Scientific and were used as received without further purification. Deionized water was used for preparing all solutions (Nanopure water purification system). Stock solutions of Pb^{2+} and Cd^{2+} were prepared by dissolving the appropriate amounts of their salts in deionized water and then diluting to various concentrations in 0.1 M acetate buffer pH 4.5 to serve as working solutions. The Nafion solution (5 wt %) was diluted to 2.5 wt % with ethanol.

Electrochemistry was done with a single-compartment three electrode glass cell containing 15 mL of solution. Platinum wire and Ag/AgCl (filled with 3 M KCl) were used as the auxiliary electrode and reference electrode, respectively. Supporting electrolyte was 0.1 M acetate buffer (pH 4.5). EIS was done with a Gamry Reference 600 potentiostat (Gamry Inc.). Impedance measurements were made at the open circuit potential relative to the Ag/AgCl reference electrode with 5.0 mM $Ru(bpy)_3Cl_2$ in 0.1 M acetate buffer (pH 4.5). An alternating potential with a 5 mV amplitude was applied in the frequency range from 0.1 to 10^6 Hz. Echem Analyst from Gamry was used to analyze the impedance spectra. The stripping voltammetry and cyclic voltammetry were done with a BASi 100B Electrochemical Analyzer from BASi. Raman spectra were acquired with a Renishaw inVia Raman microscope system. Scanning electron micrographs (SEMs) were obtained using an EVEX mini-SEM, SX-3000 or ESEM, XL30 (Philips). The energy dispersive X-ray spectroscopy (EDX) was done on the ESEM, XL30.

Preparation of Electrospun Carbon Nanofibers from PAN. For electrospinning, a PAN polymeric solution was prepared by dissolving 11 wt % of PAN in DMF solvent that then was constantly fed to the needle at 1.0 mL/h using a syringe pump. The high voltage ~16−18 kV was applied across a gap of 25 cm between the nozzle tip and the aluminum foil collector. Total dispensed volume of PAN solution was 400 μL for each sample. To maintain the fiber morphology at elevated temperature, electrospun PAN fiber membranes were stabilized at 280 °C for 3 h at a heating rate of 2 °C/min in the air. After stabilization, PAN membranes were carbonized at 1000 °C for 1 h with a heating rate of 5 °C/min in an ultrahigh purity argon gas environment.

Electrode Preparation. Prior to use, the GC electrode (BASi) was polished with 0.05 μm alumina on a polishing cloth (catalog no. 40-7218, Buehler Co.), cleaned in an ultrasonicated bath of doubly distilled H_2O for 5 min, rinsed with doubly distilled H_2O, and dried with compressed air. CNFs as prepared consisted of a 2.5 cm × 5 cm mat of one continuous fiber. To prepare each electrode, a piece of the mat was cut off, and then ultrasonic agitation for ~30 min was used to disperse the CNFs into a 2.5 wt % Nafion-ethanol solution to give a 1.0 mg/mL Nafion-CNF suspension that was used unless specified otherwise. During this process, the long CNFs broke into shorter fibers. Next, 20 μL of the mixture was placed on the surface of the GC electrode and solvent was evaporated in the air at room temperature.

Analysis Procedure. Stripping analysis consists of two main steps: accumulation and stripping. The accumulation time or deposition time was 5 min unless specified otherwise. After depositing metals on a CNF/Nafion/GC electrode, the reduced metals were stripped off using Osteryoung square-wave stripping voltammetry (OSWSV): step potential = 4 mV; S. W. amplitude = 25 mV; frequency = 15 Hz. The stripping peak currents were used to quantify the metals after baseline correction by the BASi. The stripping peak potentials were used to assign the metals. Prior to each measurement, the electrode was cleaned at 800 mV for 150 s to remove any deposit from the previous measurement.

RESULTS AND DISCUSSION

Electrode Characterization. SEMs of representative morphologies of the as-electrospun, stabilized, low temperature (1000 °C) carbonized PAN nanofiber bundles are shown in Figure 1a,b. As shown in the figure, the PAN-CNFs are straight

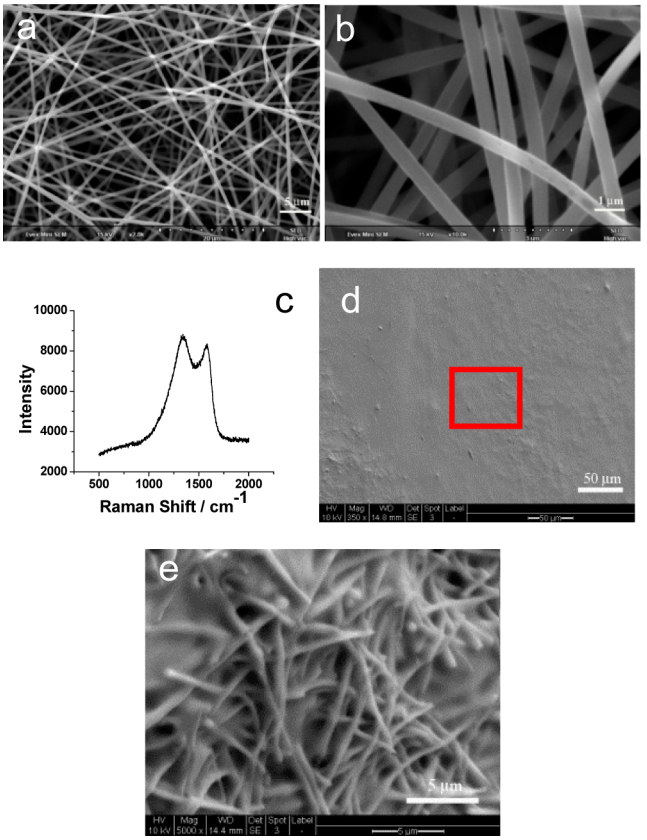

Figure 1. SEMs of electrospun PAN fibers after calcination at 1000 °C for 1 h: (a) at low magnification, (b) at high magnification, (c) Raman spectrum of part a, SEMs of CNF/Nafion/GC electrode surface with 1.0 mg CNF/mL Nafion (d) at low magnification and (e) at high magnification.

rod shapes with diameters of 450 ± 25 nm and are randomly oriented. The PAN-CNFs are uniform without microscopically identifiable beads and/or beaded nanofibers.

The Raman spectrum of the carbonized PAN nanofibers shows two characteristic bands centered at 1338 and 1587 cm^{-1} (Figure 1c). The band at 1338 cm^{-1} is the well-known D band, which is related to disordered or turbostratic carbonaceous structures. The band centered at 1587 cm^{-1} is due to the E_{2g2} C═C stretching vibration (G band), which is highly related to ordered graphitic structures. The integrated Raman intensity I_D and I_G are proportional to the number of the scattering disordered and ordered sp^2 bonding carbon atoms in the illuminated area. Therefore, the relative intensity ratio of the D-

DOI: 10.1021/acs.analchem.5b02017
Anal. Chem. XXXX, XXX, XXX−XXX

band to the G-band I_D/I_G (defined as the *R*-value) depends on the degree of graphitization and alignment of the graphitic planes. A smaller *R* value indicates a higher amount of sp^2 (graphite) clusters on the sample. The *R* value for our PAN-CNFs is 1.05, which is smaller than reported for other PAN-CNFs (1.39−2.67) under similar conditions.[18−20] This shows that our PAN-CNFs have a higher ratio of ordered graphite structures. The relationship of the *R*-value and the crystallite domain size L_a, i.e., L_a (nm) = 4.4/*R*, has been developed by Knight and White.[21] On the basis of this relationship, L_a was estimated to be 4.2 nm.

During the search for an electrode preparation procedure, the CNFs were found to be difficult to work with as free-standing electrodes. Consequently, a glassy carbon electrode was used as a substrate to provide mechanical stability and to serve as a means for making electrical contact with a CNF coating. The intent was to cover the GC surface with a sufficiently thick coating of CNFs that covers up the underlying GC surface and transforms it into a CNF electrode. Although the hydrophobic CNFs adhered reasonably well to each other and to the underlying GC, adhesion was insufficient to provide rugged electrodes that did not lose CNFs during experimentation. Consequently, we used Nafion as an adhesive to stabilize the CNFs on the surface of the GC electrode. Nafion served well for this purpose and enabled reproducible and reliable electrodes to be made. Because Nafion is a cation exchanger, it should not interfere with the electrochemical processes for positively charged metal ions such as Pb^{2+} and Cd^{2+} involved in ASV. The resulting electrode is analogous to the carbon nanotube (CNT)-loaded Nafion film sensor that we developed for the detection of metal ions such as europium by preconcentration voltammetry.[22]

An SEM of the CNF/Nafion/GC electrode at low magnification (Figure 1d) shows the GC to be uniformly covered with a coating of CNF/Nafion that has a textured finish. Higher magnification (Figure 1e) shows individual CNFs with a thin coating of Nafion to be aligned on the surface randomly and stacked on each other. These CNFs are sufficiently dense to be electrically contacting each other and to form an extension of the underlying GC electrode. After sonication, we observed that the lengths of the CNFs were shorter compared to the as-obtained CNFs. The surface of the CNF/Nafion/GC is different from that of our previously reported CNT/Nafion/GC electrode in that the latter was a dispersion of smaller CNTs in a film of Nafion without gaps,[22] whereas this new material can be described as longer fibers stacked on the GC and individually coated with Nafion, which serves to adhere them together. This difference in morphology is due to the difference in length and diameter for the CNFs compared to the CNTs. The diameters of CNFs are 450 ± 25 nm and the lengths are up to several micrometers. In contrast, the CNTs were only 150 ± 50 nm in length and 6−10 graphite layers thick in diameter. After coating, the diameters of CNF/Nafion are 600 ± 80 nm and the thickness of Nafion film is around 75 nm on the individual CNFs.

The electrochemical behavior of the fabricated electrodes was first studied by cyclic voltammetry using $Ru(bpy)_3^{2+}$ as a reversible redox couple model. We used 0.1 M acetate buffer (pH 4.5) as the supporting electrolyte for all experiments because it has been found to be exceptionally good for ASV of heavy metals.[10−13,23] Figure 2 shows cyclic voltammograms (CVs) of 5.0 mM $Ru(bpy)_3^{2+}$ at a CNF/Nafion/GC electrode, a Nafion/GC, and a GC electrode in an acetate buffer solution at a scan rate 100 mV/s. Before the measurements, the CNF/Nafion/GC and Nafion/GC electrodes were immersed in the 5.0 mM $Ru(bpy)_3^{2+}$

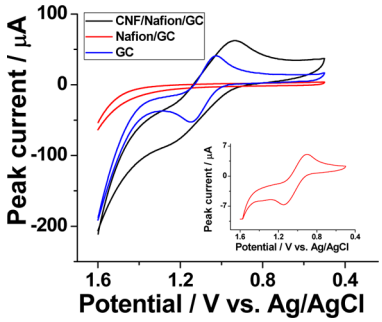

Figure 2. Comparison of CVs at CNF/Nafion/GC, Nafion/GC electrode (also expanded scale in inset), and GC electrode at a scan rate of 100 mV/s in 5.0 mM $Ru(bpy)_3^{2+}$, 0.1 M acetate buffer pH 4.5.

solution for 1 h with stirring to evaluate possible uptake by the Nafion film. In the case of GC and Nafion/GC electrodes, the voltammograms display well-defined voltammetric waves with near-equal anodic and cathodic peaks (Figure 2 and inset). However, the peak currents on GC are significantly smaller after coating with Nafion film. The usual enhancement in current provided by $Ru(bpy)_3^{2+}$ partitioning into Nafion is not observed.[24] We attribute this to the acidic buffer which provides protons to compete with $Ru(bpy)_3^{2+}$ for the negatively charged sulfonic acid sites in the film. The peak currents are significantly larger on CNF/Nafion/GC compared to the Nafion/GC electrode, which indicates that the modification with CNFs provided the conducting bridges to greatly expand the surface area for the electron transfer of $Ru(bpy)_3^{2+}$, as reported previously for the voltammetry of Eu^{3+} at a CNT/Nafion/GC electrode.[22] From CV, the peak currents are 50 times larger at a CNF/Nafion/GC electrode (1.0 mg/mL) compared to those at a Nafion/GC electrode and 5 times greater than at a bare GC electrode (Figure 2). The enhancement of the anodic/cathodic current is due to the increased electrode surface area for the CNF/Nafion/GC electrode. The peak to peak separation for the bare GC is 100 mV (E_{pa} at 1.04 V, E_{pc} at 1.14 V), and 240 mV for Nafion/GC (E_{pa} at 0.91 V, E_{pc} at 1.15 V, Figure 2 inset), whereas, the peak to peak separation is 260 mV for the CNF/Nafion/GC electrode (E_{pa} at 0.96 V, E_{pc} at 1.22 V) under the same conditions. The wider peak to peak separation is attributed primarily to Ohmic potential drop of the CNFs. These experiments show the Nafion film is serving primarily as an adhesive to hold the CNFs together on the GC surface and is not contributing to preconcentration of the positively charged $Ru(bpy)_3^{2+}$ because of the low pH. Thicker films impede the voltammetry as shown for the Nafion/GC electrode compared to bare GC, but this effect would be minimal for the CNF/Nafion/GC electrode because the coating on the CNFs is very thin as seen in Figure 1e.

To further characterize the electrode, the effect of scan rate on the CV behavior of the CNF-modified electrode was investigated (Figure S1a). When the scan rate increases from 5 to 500 mV/s, the oxidation peak potential gradually shifts to a more positive potential, whereas, the reduction peak potential shifts to a negative potential, and correspondingly, the peak separation increases from 110 mV to 420 mV. The peak current increases linearly with square root of the scan rate. This indicates that the electron transfer process is diffusion controlled and further confirms that the $Ru(bpy)_3^{2+}$ is not accumulating in the Nafion film, which would give restricted diffusion behavior. The correlation equations are $I_{pc} = (121.0 \pm 1.3)x + (19.2 \pm 0.5)$ ($R^2 = 0.999$) and $I_{pa} = (-79.3 \pm 0.8)x - (10.5 \pm 0.3)$ (R^2 =

DOI: 10.1021/acs.analchem.5b02017
Anal. Chem. XXXX, XXX, XXX−XXX

0.998), where x is the square root of scan rate $(V/s)^{1/2}$ and uncertainties are standard deviation, hereinafter (Figure S1b).

The electrochemical behavior of the fabricated electrodes was then studied by cyclic voltammetry in supporting electrolyte only. The featureless cyclic voltammogram obtained at a bare GC electrode in 0.1 M acetate buffer (pH 4.5) and the large gap between the forward and reverse scan obtained at a CNF/Nafion/GC electrode and Nafion/GC electrode, shown in Figure S2, indicate typical electrical double layer capacitive behavior. It can be seen that the presence of the Nafion film on the GC electrode minimally affects the capacitance current compared to the bare electrode. However, the presence of CNFs greatly increases the capacitance current, which is expected because the electrode surface area is significantly larger. The enhanced capacitive current for the CNF/Nafion/GC electrode suggests good charge propagation within the CNFs. The double layer capacitance is generated at the CNF/Nafion and CNF/Nafion/electrolyte interfaces and determined by the effective surface of the electrode and dielectric constant of the electrolyte.[22,25] The specific capacitance (Cs) of the CNF/Nafion/GC electrode is calculated to be 10.6 F/g at 0.1 V/s (calculation of C_s is in the Supporting Information), which is higher than 5.0 F/g at the superaligned CNTs used in a capacitor[26] and 3.4 F/g at a CNT modified GC electrode under similar conditions.[22] The higher capacitance is due to the large surface area created by the CNFs in the Nafion.[27,28]

EIS was used to investigate the impedance changes at the electrode surface caused by the modification process and the effect of the ratio of CNFs to Nafion (expressed as weight of CNFs to volume of Nafion solution, mg/mL) in the preparation used to coat the GC (Figure 3). Figure 3a shows the Randle's equivalent circuit used to fit the impedance data.[22,29,30] The circuit is made up of solution resistance (R_s) which contains the resistance of supporting electrolyte and the electrode film (CNFs and Nafion) resistance, the charge transfer resistance of the electrochemical reactions of the redox couple (R_{ct}), the CPE corresponding to the double layer capacitance (C_{dl}) of the electrode (Z_Q), and the finite thickness Warburg diffusion impedance of $Ru(bpy)_3^{2+}$ for the electrode (Z_O). (Detailed information about the model equivalent circuit is included in the Supporting Information, and the fitting values of the parameters are summarized in Table S1.)

Figure 3b shows the effect of varying concentrations of CNFs in Nafion on the commonly used Nyquist plot, which includes a semicircular part and a linear part. The major effect of increasing the concentration of CNFs in the Nafion is the dramatic depression in the semicircle part of the plot, which indicates that R_{ct} is decreasing. As shown in Table S1, R_{ct} decreases from 4971 Ω with Nafion only to 572.9 Ω with 1.0 mg/mL of CNFs. Increasing the ratio CNF/Nafion results in an increase in the electrode/electrolyte interfacial area and a thinner Nafion film on individual CNFs, which reduces the energy barrier for the ion transfer between the coating and the electrolyte.[31] Depressed semicircles can be attributed to the electrode porosity, electrode inhomogeneity, and surface roughness as well as variation in thickness of the surface coating as seen in Figure 1e. In the lower ratio range of CNF/Nafion, R_{ct} (Table S1) significantly decreased with increasing CNF/Nafion up to a concentration of 0.50 mg CNF/mL Nafion compared to the Nafion/GC electrode. R_{ct} then decreased more slowly over the higher CNF/Nafion ratio range of 0.5−1.0 mg/mL. This behavior is different from that in our earlier report on the CNT/Nafion/GC electrode, where the decrease in R_{ct} is small in the lower ratio range from 0 to 0.25 mg CNF/mL Nafion and large in the higher concentration range of 0.5−1.0 mg CNF/mL Nafion. This difference in behavior is attributed to the difference in lengths of the CNFs compared to the CNTs. The longer CNFs are electrically contacting each other even at low ratios of CNF/Nafion, whereas, CNTs disperse in the film of Nafion without contacting each other in the lower concentration range. Therefore, the CNTs need to reach a critical concentration to effectively contact each other and become an extension of the GC electrode, which is not the case with the CNFs used in this study. Also, the double layer capacitance (C_{dl}) of the electrode (Z_Q) shows a sharp increase from 0 mg CNF/mL Nafion to 0.25 mg CNF/mL Nafion (Table S1), which is consistent with a large increase in electrode surface area caused by the CNFs at the lowest concentration. The depressed semicircles (Z_{re}) and typical angles between 45 and 90° (Z_{im}) in the Nyquist plots suggest that the nonideal capacitor known as constant phase

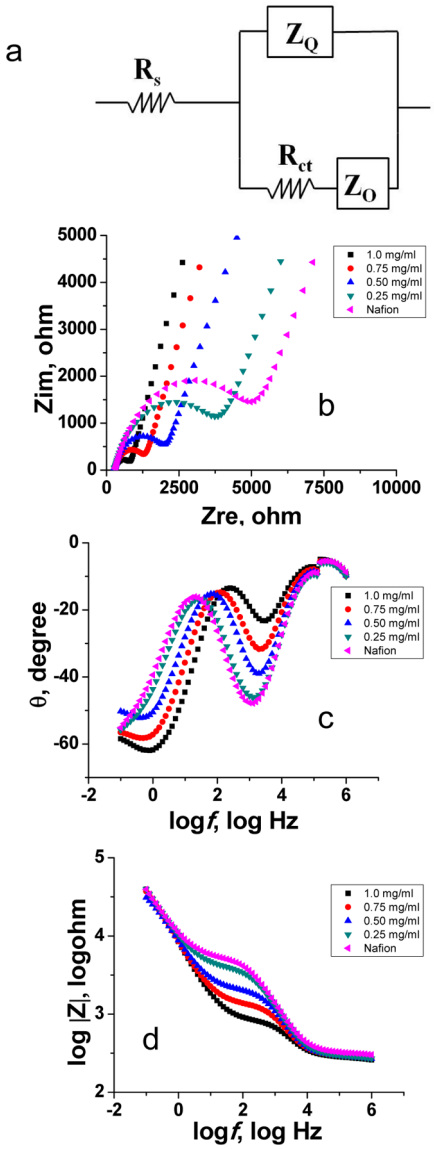

Figure 3. (a) Equivalent circuit for CNF/Nafion/GC electrode, (b) Nyquist plots for varying concentrations of CNFs in Nafion solution and (c,d) Bode plots of 5.0 mM $Ru(bpy)_3^{2+}$ in 0.1 M acetate buffer with the CNF/Nafion/GC electrode. The electrode was soaked in the 5.0 mM $Ru(bpy)_3^{2+}$ for 1 h with stirring before measurement.

DOI: 10.1021/acs.analchem.5b02017
Anal. Chem. XXXX, XXX, XXX−XXX

element (CPE) is present. The linear segment at lower frequencies corresponds to capacitive behavior of the finite thickness diffusion process.[22,31] The slopes of these straight lines from the Nyquist plots hardly change with the variation in CNF concentration, which suggests that the model of the composite film does not change with the increase of the film thickness. In other words, the film thickness does not affect the reliability of the equivalent circuit.

Bode plots confirm the results obtained from the Nyquist plots. Bode plots in the form of phase angle (θ) versus frequency ($\log f$) are characterized by one well-defined peak corresponding to one distinct relaxation process (Figure 3c).[31] A near-zero phase shift was obtained in the higher frequency region, which indicates the electrode behaves primarily as a resistor due to the solution/film resistance. In the intermediate frequencies, the capacitive behavior shows up causing the increased phase angle. In these frequencies, charge transfer between CNF-Nafion and $Ru(bpy)_3^{2+}$ occurred, resulting in the well-defined peak that is significantly influenced by the concentration of CNFs in the Nafion. In addition, it can be seen that the phase angle only changes a little at 0.25 mg CNF/mL Nafion compared to the Nafion only modified electrode. When the ratio of CNFs increased to 0.5 mg/mL Nafion, the phase angle greatly decreases, which is consistent with the Nyquist plot. Bode plots of impedance $\log |Z|$ vs $\log f$ (Figure 3d) have two plateaus. Compared to the CNT/Nafion/GC electrode in 1.0 mM $Fe(CN)_6^{3-}$ solution under similar conditions, a second plateau in the intermediate and low frequencies region appears, which suggests a diffusion controlled process for $Ru(bpy)_3^{2+}$ within the film. This is consistent with the CV results (Figure S1). When the concentration of CNFs increases, $\log |Z|$ decreases and capacitance increases ($Z = -j/\omega C$; where $j^2 = -1$, ω is the angular frequency, and C is the capacitance), which also shows that CNF concentration plays an important role in the capacitive behavior.

Optimization of Detection of Pb^{2+} and Cd^{2+} with CNF/Nafion/GC Electrode by ASV. Pb^{2+} and Cd^{2+} were chosen as representative of toxic heavy metal ions commonly determined by stripping voltammetry to evaluate the performance of the CNF/Nafion/GC electrode using ASV. Osteryoung square wave voltammetry was used for the stripping step in all experiments.

Deposition potential is one of the important parameters for stripping analysis. Figure S3 shows the effects of deposition potential on the stripping peak currents of 0.2 μM Pb^{2+} and 0.6 μM Cd^{2+} in separate experiments with a deposition time of 5 min. The deposition for Pb and Cd begins when the potential reached −0.9 V and reaches a maximum at −1.25 V based on the stripping current. The decrease in peak current at the most negative deposition potentials is attributed to the onset of hydrogen evolution at the electrode. The evolution of hydrogen influences the availability of active electrode surface and interferes with mass transport of metal ions during metal deposition. An optimized deposition potential −1.25 V was chosen for the detection of Pb^{2+} and Cd^{2+} for maximum peak current response.

The effect of the deposition time (1−8 min) on the anodic stripping peak currents of Pb^{2+} and Cd^{2+} is shown in Figure S4. The peak current for Pb^{2+} detection at the modified electrode increases rapidly during the accumulation time up to 5 min and then tends to increase more gradually because of the limited active sites for deposition. A similar trend is observed for Cd^{2+} detection, although the peak current increases rapidly only up to 6 min. Although increasing the accumulation time significantly improves the sensitivity, it also lowers the upper range in concentration due to the rapid surface saturation at high Pb^{2+} and Cd^{2+} concentrations. Therefore, to achieve a wider response range, 5 min was chosen as the accumulation time for the following experiments.

Effect of CNFs on Heavy Metal Ion Detection. The effects of CNFs and Nafion on the determination of the heavy metal ions were investigated by stripping voltammetry. It can be seen from Figure 4 that the CNF/Nafion/GC electrode shows a

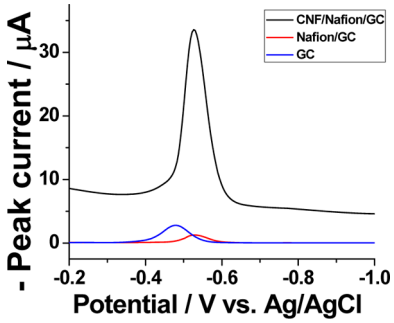

Figure 4. Stripping voltammograms for 0.5 μM Pb^{2+} in 0.1 M acetate buffer at the CNF/Nafion/GC electrode, Nafion/GC electrode, and GC electrode. Deposition potential, −1.25 V; deposition time, 5 min.

significant increase in both the peak current for the stripping voltammetry of Pb and the background current compared to bare GC and Nafion/GC electrodes.

The peak current for the CNF/Nafion/GC electrode is 20 and 8 times higher than for the Nafion/GC and bare GC electrodes, respectively. The larger peak current for CNF/Nafion/GC electrode means that the sensitivity for Pb^{2+} is improved. At the same time, the ratio of S/N is improved 20 times compared to the GC electrode, which means an improved limit of detection. The higher peak current for the CNF/Nafion/GC electrode is due to the larger active surface area of the CNFs compared to the bare GC and Nafion/GC electrode. The stripping peak potential for Pb^{2+} shifts 52 mV negatively for Nafion/GC electrode and CNF/Nafion/GC (both at −530 mV) compared to the bare GC electrode (−478 mV). The peak potential shift is attributed to Coulombic interactions between the cation-exchanging Nafion film and the accumulated metal ions, affecting the redox potential of the latter.[32]

Individual Metal Ion Detection. Under the optimized conditions, the CNF/Nafion modified GC electrode was applied to the determination of Pb^{2+} and Cd^{2+} by ASV. Well-defined stripping peaks were obtained for both Pb^{2+} and Cd^{2+}, respectively (Figure 5). The peak current increases linearly versus Pb^{2+} and Cd^{2+} concentration; the correlation equations are $I_p = (57.8 \pm 2.5)C - (4.2 \pm 1.1)$ ($R^2 = 0.990$) and $I_p = (13.8 \pm 0.4)C - (4.4 \pm 0.5)$ ($R^2 = 0.995$) for Pb^{2+} and Cd^{2+}, respectively. Here, I_p is the stripping peak current (μA) and C is the concentration of Pb^{2+} or Cd^{2+} (μM). From the slopes of the calibration plots, the sensitivity is higher for Pb than Cd. The relative peak current for Cd is 11.8% compared to Pb set as 100% at the same concentration of 0.6 μM; the stripping peak currents are 31.25 μA and 3.68 μA for Pb^{2+} and Cd^{2+}, respectively. Potentials of the stripping peak are −522 mV for Pb, −786 mV for Cd. The calculated detection limits (based on the 3σ method) are 0.9 nM and 1.5 nM for Pb^{2+} and Cd^{2+}, respectively. These detection limits are well below the allowable limits in drinking water instituted by the World Health Organization (WHO) (Pb 24.1 nM, Cd 20.76 nM).[33] The CNF/Nafion/GC electrode

DOI: 10.1021/acs.analchem.5b02017
Anal. Chem. XXXX, XXX, XXX−XXX

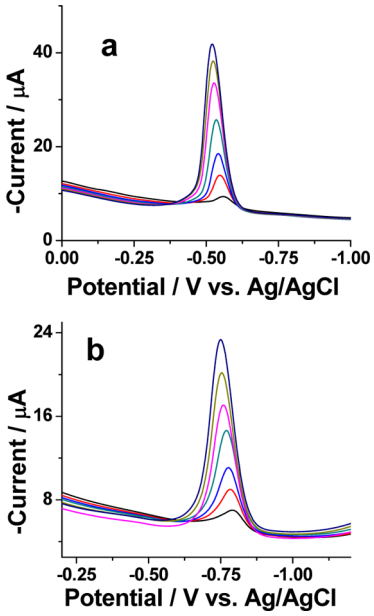

Figure 5. OSWSV stripping voltammograms for Pb^{2+} and Cd^{2+} in 0.1 M acetate buffer at CNF/Nafion/GC electrode (a) 0.1, 0.2, 0.3, 0.4, 0.5, 0.6, and 0.7 μM Pb^{2+} and (b) 0.4, 0.6, 0.8, 1.0, 1.2, 1.4, and 1.6 μM Cd^{2+}.

shows higher sensitivity and lower detection limits compared to other materials-modified glassy carbon electrodes. For example, the detection limit for Pb and Cd is 1.0 and 4.4 nM on an ionic liquid (1-ethyl-3-methylimidazolium tetracynoborate)/Nafion/GC electrode.[34] Huang et al. reported the Co_3O_4/Nafion modified GC electrode with a detection limit for Pb of 18 nM.[35] The detection limits for Cd on the CNT/Nafion and bismuth/Nafion modified GC are 6 nM and 7.8 nM, respectively.[36,37] From the above analysis, the CNFs improve the sensitivity for the detection of heavy metal ions and lower the detection limit. In our case, the sensitivity to Pb is higher than Cd, which is similar to the CNT modified GC electrode. This higher sensitivity is strongly related to the composition of the electrode.[11−13,38,39] For example, Fe_3O_4-reduced graphene oxide nanoparticle, polyaniline coating, CNT, and CNT/Nafion/bismuth composite modified GC electrodes all show higher sensitivity to Pb compared to Cd.[40−43] However, several other research groups reported the reverse observation. For example, Nafion-Graphene composite film modified GC electrodes and bismuth/polyaniline/GC electrodes show higher sensitivity for Cd than Pb.[23,44] Taken all together, the higher sensitivity to Pb is highly related to the composition of the CNF/Nafion/GC electrode and its effect on the rate of electron transfer.

Simultaneous Detection of Pb and Cd. Figure 6 shows the simultaneous determination of Pb^{2+} and Cd^{2+} in a mixture under the optimized conditions. The peak currents increase linearly versus the concentration of Pb^{2+} and Cd^{2+} and the correlation equations are $I_p = (52.2 \pm 2.6)C - (3.0 \pm 0.9)$ ($R^2 = 0.991$) and $I_p = (12.0 \pm 0.4)C - (1.5 \pm 0.3)$ ($R^2 = 0.996$), respectively. Compared to their corresponding individual metal ion detection, the sensitivities slightly decreased. The slope changes of these calibration plots suggest that interactions among the deposited metals cause the sensitivity change compared to the determination of the individual metal ions (Figure 5 and Figure 6). Potentials of the stripping peaks are at −546 mV for Pb and −778 mV for Cd when the concentration of Cd is at 0.6 μM, and Pb at 0.3 μM. Although there is some interaction between the

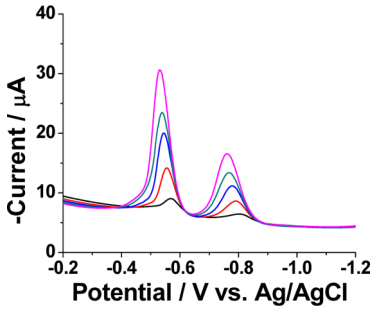

Figure 6. OSWSV stripping voltammograms for simultaneous detection of Pb^{2+} and Cd^{2+} at the CNF/Nafion/GC electrode, concentrations: 0.1, 0.2, 0.3, 0.4, 0.5 μM Pb^{2+} and 0.2, 0.4, 0.6, 0.8, 1.0 μM Cd^{2+}.

deposited Cd and Pb, these two metals are still detectable simultaneously.

Interactions Between Deposited Pb and Cd. To further understand the metal deposition process, CNF/Nafion/GC electrodes with large amounts of metal deposited on them were investigated by SEM and SEM-EDX. Pb and Cd ions were deposited at −1.25 V for 1 h from 0.2 mM Pb^{2+} and 0.3 mM Cd^{2+} solution. Figure 7 shows SEMs of the deposited Pb and Cd on

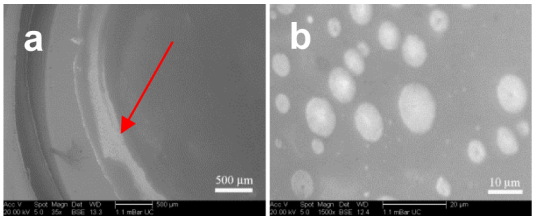

Figure 7. (a) SEMs of CNF/Nafion/GC electrode after deposition from 0.2 mM Pb^{2+} and 0.3 mM Cd^{2+} solution for 1 h. The depostion potential was −1.25 V. (b) Magnification of the edge area of part a.

the surface of CNF/Nafion/GC electrode. From the SEMs, it can be seen that a visually uniform deposit of the Pb and Cd forms on the center area of the electrode surface (Figure 7a); in contrast, thicker metal particles deposit on the edge of the CNF/Nafion/GC electrode (Figure 7b). This phenomenon is only observed at such high concentration and long deposition time. This is due to the planar diffusion controlled process at the electrode center and increased mass transport from the "edge effect" at the electrode edge which results in more metal ions being reduced there. Figure S5a,b shows the SEM-EDX for the deposited Pb and Cd. In the edge region, the Pb and Cd weight percentages (Pb, 10.57%; Cd, 2.75% weight percentage) are higher compared to the electrode center (Pb, 4.63%; Cd, 1.40% weight percentage) (Figure S5, Table S2). The above results are consistent with the broad stripping peak due to multiple layers of metals depositing on the electrode surface.

CONCLUSION

An electrospun CNF/Nafion functionalized glassy carbon electrode was successfully used for the simultaneous detection of heavy metal ions. The CNFs greatly increase the sensitivity and lower the detection limit compared to bare GC and Nafion/GC electrodes. CNF/Nafion/GC electrodes exhibit a greater capacitance compared to bare GC and Nafion/GC because of the increased surface area. The EIS study shows that the ratio of CNF/Nafion plays an important role in the electrochemical behavior. The metal deposition process for the codeposited Pb−

DOI: 10.1021/acs.analchem.5b02017
Anal. Chem. XXXX, XXX, XXX−XXX

Cd alloys forms a uniform layer at the electrode center, and particles appear at the electrode edge area at high concentrations. Lower detection limits for ASV were obtained than those reported for other materials-modified glassy carbon electrodes.

■ ASSOCIATED CONTENT

Supporting Information

This material is available free of charge via the Internet at http://pubs.acs.org/. The Supporting Information is available free of charge on the ACS Publications website at DOI: 10.1021/acs.analchem.5b02017.

Voltammetry results, surface analysis, mathematical expressions, and fitting values of components in the model equivalent circuit (PDF)

■ AUTHOR INFORMATION

Corresponding Author

*E-mail: William.Heineman@uc.edu. Phone: 01-513-556-9210. Fax: 01-513-556-9329.

Notes

The authors declare no competing financial interest.

■ ACKNOWLEDGMENTS

The authors thank the University of Cincinnati (Research Council-Renewable Energy Grant) and the National Science Foundation (NSF Grant ERC 0812348) for financial support. We also thank Dr. Necati Kaval for the SEM and EDX analysis.

■ REFERENCES

(1) Zhang, B.; Yu, Y.; Xu, Z.; Abouali, S.; Akbari, M.; He, Y.; Kang, F.; Kim, J. K. *Adv. Energy Mater.* **2014**, *4*, 1301448.
(2) Han, D.; Steckl, A. J. *ACS Appl. Mater. Interfaces* **2013**, *5*, 8241−8245.
(3) Han, D.; Filocamo, S.; Kirby, R.; Steckl, A. J. *ACS Appl. Mater. Interfaces* **2011**, *3*, 4633−4639.
(4) Kim, C.; Choi, Y. O.; Lee, W. J.; Yang, K. *Electrochim. Acta* **2004**, *50*, 883−887.
(5) Mathur, R. B.; Maheshwari, P. H.; Dhami, T. L.; Sharma, R. K.; Sharma, C. P. *J. Power Sources* **2006**, *161*, 790−798.
(6) Chun, I.; Reneker, D. H.; Fong, H.; Fang, X.; Deitzel, J.; Tan, N.; Kearns, K. *J. Adv. Mater.* **1999**, *31*, 36−41.
(7) Chen, L.; Hong, S.; Zhou, X.; Zhou, Z.; Hou, H. *Catal. Commun.* **2008**, *9*, 2221−2225.
(8) Long, J. W.; Dunn, B.; Rolison, D. R.; White, H. S. *Chem. Rev.* **2004**, *104*, 4463−4492.
(9) Wang, J.; Lu, J. M.; Anik, U.; Hocevar, S. B.; Ogorevc, B. *Anal. Chim. Acta* **2001**, *434*, 29−34.
(10) Wang, J.; Lu, J.; Hocevar, S. B.; Farias, P. A. M.; Ogorevc, B. *Anal. Chem.* **2000**, *72*, 3218−3222.
(11) Zhao, D.; Guo, X.; Wang, T.; Alvarez, N.; Shanov, V. N.; Heineman, W. R. *Electroanalysis* **2014**, *26*, 488−496.
(12) Guo, X.; Lee, W.; Alvarez, N.; Shanov, V. N.; Heineman, W. R. *Electroanalysis* **2013**, *25*, 1599−1604.
(13) Guo, X.; Yun, Y.; Shanov, V. N.; Halsall, H. B.; Heineman, W. R. *Electroanalysis* **2011**, *23*, 1252−1259.
(14) Wang, T.; Schlueter, K. T.; Riehl, B. L.; Johnson, J. M.; Heineman, W. R. *Anal. Chem.* **2013**, *85*, 9486−9492.
(15) Wang, T.; Manamperi, H. D.; Yue, W.; Riehl, B. L.; Riehl, B. D.; Johnson, J. M.; Heineman, W. R. *Electroanalysis* **2013**, *25*, 983−990.
(16) Jarup, L. *Br. Med. Bull.* **2003**, *68*, 167−182.
(17) Aragay, G.; Pons, J.; Merkoci, A. *Chem. Rev.* **2011**, *111*, 3433−3458.
(18) Kim, C.; Park, S. H.; Cho, J. K.; Lee, D. Y.; Park, T. J.; Lee, W. J.; Yang, K. S. J. *J. Raman Spectrosc.* **2004**, *35*, 928−933.
(19) Zhou, Z.; Lai, C.; Zhang, L.; Qian, Y.; Hou, H.; Reneker, D. H.; Fong, H. *Polymer* **2009**, *50*, 2999−3006.
(20) Wang, Y.; Serrano, S.; Santiago-Aviles, J. J. *Synth. Met.* **2003**, *138*, 423−427.
(21) Knight, D. S.; White, W. B. *J. Mater. Res.* **1989**, *4*, 385−393.
(22) Wang, T.; Zhao, D.; Guo, X.; Correa, J.; Riehl, B. L.; Heineman, W. R. *Anal. Chem.* **2014**, *86*, 4354−4361.
(23) Li, J.; Guo, S.; Zhai, Y.; Wang, E. *Anal. Chim. Acta* **2009**, *649*, 196−201.
(24) Kaval, N.; Seliskar, C. J.; Heineman, W. R. *Anal. Chem.* **2003**, *75*, 6334−6340.
(25) Stoller, M. D.; Park, S. J.; Zhu, Y.; An, J. H.; Ruoff, R. S. *Nano Lett.* **2008**, *8*, 3498−3502.
(26) Zhou, R.; Meng, C.; Zhu, F.; Li, Q.; Liu, C.; Fan, S.; Jiang, K. *Nanotechnology* **2010**, *21*, 345701.
(27) Zhang, H.; Cao, G.; Yang, Y. *Nanotechnology* **2007**, *18*, 195607.
(28) Zhang, H.; Cao, G.; Yang, Y.; Gu, Z. *J. Electrochem. Soc.* **2008**, *155*, K19−K22.
(29) Ma, X.; Xu, Z.; Yuan, H.; He, Y.; Xiao, D.; Choi, M. M. F. *Sens. Actuators, B* **2010**, *147*, 152−158.
(30) Retter, U.; Widmann, A.; Siegler, K.; Kahlert, H. *J. Electroanal. Chem.* **2003**, *546*, 87−96.
(31) Hu, C.; Yuan, S.; Hu, S. *Electrochim. Acta* **2006**, *51*, 3013−3021.
(32) Kefala, G.; Economou, A.; Voulgaropoulos, A. *Analyst* **2004**, *129*, 1082−1090.
(33) http://whqlibdoc.who.int/publications/2011/9789241548151_eng.pdf.
(34) Yang, D.; Wang, L.; Chen, Z. L.; Megharaj, M.; Naidu, R. *Electroanalysis* **2014**, *26*, 639−647.
(35) Liu, Z.; Chen, X.; Liu, J.; Huang, X. *Electrochem. Commun.* **2013**, *30*, 59−62.
(36) Sun, D.; Xie, X.; Cai, Y. P.; Zhang, H.; Wu, K. *Anal. Chim. Acta* **2007**, *581*, 27−31.
(37) Wang, Y.; Liu, Z.; Yao, G.; Zhu, P.; Hu, X.; Xu, Q.; Yang, C. *Talanta* **2010**, *80*, 1959−1963.
(38) Li, M.; Gou, H.; Al-Ogaidi, I.; Wu, N. *ACS Sustainable Chem. Eng.* **2013**, *1*, 713−723.
(39) Viry, L.; Derre, A.; Garrigue, P.; Sojic, N.; Poulin, P.; Kuhn, A. *J. Nanosci. Nanotechnol.* **2007**, *7*, 3373−3377.
(40) Sun, Y.; Chen, W.; Li, W.; Jiang, T.; Liu, J.; Liu, Z. *J. Electroanal. Chem.* **2014**, *714*, 97−102.
(41) Wang, Z.; Liu, E.; Zhao, X. *Thin Solid Films* **2011**, *519*, 5285−5289.
(42) Wu, K.; Hu, S.; Fei, J.; Bai, W. *Anal. Chim. Acta* **2003**, *489*, 215−221.
(43) Xu, H.; Zeng, L.; Xing, S.; Xian, Y.; Shi, G. *Electroanalysis* **2008**, *20*, 2655−2662.
(44) Wang, Z.; Guo, H.; Liu, E.; Yang, G.; Khun, N. W. *Electroanalysis* **2010**, *22*, 209−215.

DOI: 10.1021/acs.analchem.5b02017
Anal. Chem. XXXX, XXX, XXX−XXX